HHS Public Access

Author manuscript

Free Radic Biol Med. Author manuscript; available in PMC 2017 October 01.

Published in final edited form as:

Free Radic Biol Med. 2016 October ; 99: 533–543. doi:10.1016/j.freeradbiomed.2016.09.013.

A Novel Mouse Model for the Identification of Thioredoxin-1 Protein Interactions

Michelle L. Booze[a], **Jason M. Hansen**[b], and **Peter F. Vitiello**[a,c,*]

[a]Children's Health Research Center, Sanford Research; Sioux Falls, SD USA 57104

[b]Department of Physiology and Developmental Biology, College of Life Sciences, Brigham Young University; Provo, UT USA 84602

[c]Department of Pediatrics, Sanford School of Medicine, The University of South Dakota; Sioux Falls, SD USA 57104

Abstract

Thiol switches are important regulators of cellular signaling and are coordinated by several redox enzyme systems including thioredoxins, peroxiredoxins, and glutathione. Thioredoxin-1 (Trx1), in particular, is an important signaling molecule not only in response to redox perturbations, but also in cellular growth, regulation of gene expression, and apoptosis. The active site of this enzyme is a highly conserved C-G-P-C motif and the redox mechanism of Trx1 is rapid which presents a challenge in determining specific substrates. Numerous in vitro approaches have identified Trx1-dependent thiol switches; however, these findings may not be physiologically relevant and little is known about Trx1 interactions in vivo. In order to identify Trx1 targets in vivo, we generated a transgenic mouse with inducible expression of a mutant Trx1 transgene to stabilize intermolecular disulfides with protein substrates. Expression of the Trx1 "substrate trap" transgene did not interfere with endogenous thioredoxin or glutathione systems in brain, heart, lung, liver, and kidney. Following immunoprecipitation and proteomic analysis, we identified 41 homeostatic Trx1 interactions in perinatal lung, including previously described Trx1 substrates such as members of the peroxiredoxin family and collapsin response mediator protein 2. Using perinatal hyperoxia as a model of oxidative injury, we found 17 oxygen-induced interactions which included several cytoskeletal proteins which may be important to alveolar development. The data herein validates this novel mouse model for identification of tissue- and cell-specific Trx1-dependent pathways that regulate physiological signals in response to redox perturbations.

Graphical Abstract

*Corresponding author. Associate Scientist, Children's Health Research Center. Sanford Research. 2301 East 60th Street North, Sioux Falls, SD, USA 57104. Tel.: +605 312-6405. fax.: (605) 312-6071. peter.vitiello@sanfordhealth.org.

The authors do not have any disclosures or potential conflicts of interests to disclose.

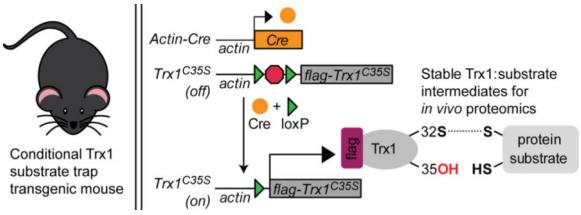

Keywords

Oxidoreductase; thioredoxin; redox signaling; oxidative stress

INTRODUCTION

Thiol switches, much like phosphorylation of serine, threonine, and tyrosine, regulate protein activity through a variety of oxidative cysteine modifications in response to intracellular and environmental signals. Thioredoxin-1 (Trx1), a fundamental oxidoreductase, is essential for cell growth and survival as deletion of this enzyme is embryonic lethal [1]. The redox action of Trx1 belies its function, a general antioxidant that maintains redox homeostasis in cellular compartments. However, Trx1 is also an important regulator of thiol switches, which indicates that it has the capacity to regulate signaling responses. Within its active site are two vicinal cysteines (Cys32/35) that lie in a cysteine-glycine-proline-cysteine orientation [2]. This “thioredoxin fold” is highly conserved throughout organismal taxa, from E. coli to modern humans [3]. The crystal structure of Trx1, resolved in the 1970s, demonstrated that the thioredoxin fold contains five pleated sheets in parallel and antiparallel orientation which are surrounded by four alpha-helices [4]. Additional crystallography studies have shown that Trx1 undergoes a conformation change when the reactive cysteines are oxidized [5]. It is the cyclical oxidation and reduction of vicinal thiols in the Trx1 active site which gives this enzyme its oxidoreductase activity. This mechanism is responsible for its intermolecular interactions with other dedicated redox cycling enzymes as well as protein substrates containing thiol switches [6]. Trx1 reduces oxidized cysteines, including disulfide bridges, in target substrates. The Cys32 residue, through nucleophilic attack, binds to the target substrate. Cys35 then reduces this bond which creates a disulfide bridge between the two cysteines within the active site of Trx1. This effectively inhibits the reducing activity of Trx1. Trx1 activity is restored when it is reduced by its partner enzyme, thioredoxin reductase-1 (TrxR1) [7]. This reaction mechanism is rapid which presents a challenge when studying Trx1 interactions both in vitro and in vivo.

One method that has been essential for elucidating novel Trx1 substrates is the use of Isotope-Coded Affinity Tags (ICAT). This method was first developed using protein lysates from fertilized barley seeds [8]. Iodoacetamide was used to block free thiols generated by Trx1-dependent reduction of disulfides in target proteins. “Light” and “heavy” carbon ICAT reagents were added to the control and experimental samples, respectively, which allowed for the measurement of Trx1-dependent reduction based upon the ratio of light to heavy ICAT carbon (control vs. experimental) via liquid chromatography-mass spectrometry. The

ICAT method has also been applied to additional models, including eukaryotic cells [9] and ventricle tissue from mice with cardiac-specific overexpression of Trx1 [10]. This method has as a distinct advantage in that not only can Trx1-dependent disulfide reduction of target substrates can be measured, but additional posttranslational modifications, such as nitrosylation by Trx1, can also be assessed [11]. However, while Trx1 substrates have been identified using ICAT, these interactions were found in vitro and may not have biological relevance.

The Trx1 substrate trap is a bona fide method to directly identify Trx1 interactions (Figure 1) [12]. For human Trx1, mutation of Cys35 to serine (C35S) replaces the highly reactive resolving thiol with a hydroxyl group thereby interrupting the oxidoreductase reaction. Therefore, the substrate trap mutation stabilizes the intermolecular disulfide between Trx1 and substrate. The Trx1 substrate trap, including variations utilizing an alanine substitution, has been used in a variety of systems to identify Trx1-dependent thiol switches. This approach identified targets of the thioredoxin-related protein DsbG in E. coli [13] and Trx1:peroxiredoxin complexes in yeast [14]. It has also been used with plant-derived recombinant thioredoxin in a test tube-based system [15, 16]. Studies from our laboratory have successfully used the Trx1 substrate trap in lung adenocarcinoma cells [17]. Novel nuclear targets, such as the transcription factor PC4 and SFRS1 interaction protein 1 (PSIP1), have been identified by fusing a canonical nuclear localization signal to the substrate trap transgene [18]. However, there are caveats with using this substrate trap in vitro or in cellular models since they do not recapitulate complex physiologies of multicellular organisms. Additionally, immortalized tumor cell lines or primary cells requiring extensive manipulations during isolation do not likely represent physiological conditions and may harbor redox perturbations [19, 20]. While results from these studies have expanded our knowledge of the interactions of Trx1, we are still lacking information on interactions of this important redox enzyme in vivo.

We have generated a transgenic mouse that expresses the human Trx1 C35S substrate trap with an N-terminal flag tag (flag-hTrx1^{C35S}). This transgene also includes a loxP-STOP-loxP cassette between the CMV early enhancer/chicken β-actin (CAG) promoter and the flag-hTrx1^{C35S} sequence which allows for spatial and temporal transgene expression. In this study, flag-hTrx1^{C35S} was ubiquitously expressed using cre recombinase driven by the β-actin promoter (actin-cre) [21]. 41 static interactions of Trx1 were identified in postnatal lung tissue, including six known substrates. With the addition of neonatal hyperoxic injury as an oxidative injury paradigm, we identified 17 oxygen-sensitive Trx1 substrates. Combined with different disease models, temporal and cell-specific expression of flag-hTrx1^{C35S} in this novel transgenic mouse will serve as an essential tool to elucidate redox-dependent Trx1 signaling in variety of tissues and disease pathologies.

MATERIALS AND METHODS

Flag-hTrx1^{C35S} Transgenic Mouse

The flag-hTrx1^{C35S} plasmid, #21285 [22], was purchased from Addgene (Cambridge, MA) and sent to Applied StemCell (Milpitas, CA) for generation of flag-hTrx1^{C35S} transgenic mice. Transgenic founders were generated in four steps. First, the founder line Rosa26-3attP

was created by knocking in three tandem attP sites into the Rosa26 locus in an FVB mouse. Second, the flag-hTrx1^{C35S} transgene was inserted into the Rosa36-3attP site. The integration cocktail, which consisted of the plasmid pBT378-attP-flag-hTrx1^{C35S}-attP and in vitro transcribed ϕC31 mRNA, was injected into the pronucleus of zygotes from heterozygous Rosa26-3attP FVB mice. The ϕC31 enzyme ensured the correct integration of the flag-hTrx1^{C35S} transgene into the 3attP locus. Third, zygotes were implanted into CD1 foster mice. Fourth, two founders were identified by PCR. FVB flag-hTrx1^{C35S} mice were crossed with C57Bl6/J mice to create generation N1. Genomic DNA was prepared from tail biopsy and genotyping was performed using the AccuStart II Mouse Genotyping Kit (Quanta Biosciences, Gaithersburg, MD) and two primer sets: 1) CAG promoter 5'-GGTGATAGGTGGCAAGTGGTATTCCGTAAG-3', 5'-CATATATGGGCTATGAACTAATGACCCCGT-3' and 2) Poly-A tail 5'-GACGATGTAGGTCACGGTCTCGAAG-3', 5'-CCGCGAAGTTCCTATACCTTTTG-3'. N1 FVB/C57Bl6/J flag-hTrx^{C35S} hemizygous mice were paired with actin-cre homozygous mice obtained from The Jackson Laboratory (Bar Harbor, ME). Offspring from these breeders were sacrificed for tissue collection between postnatal days 5 and 7 (PND5–7).

Hyperoxia Treatment

All animal experiments were conducted with approval from the Sanford Research Institutional Animal Care and Use Committee. Sanford Research has an Animal Welfare Assurance on file with the Office of Laboratory Animal Welfare (A-4568-01) and is a licensed research facility under the authority of the United Sates Department of Agriculture (46-R-0011). Actin-cre;flag-hTrx1^{C35S} and actin-cre newborn mice litters (PND<0.5) were randomly placed in 85% oxygen or room air the first seven days of life [23]. Oxygen concentration was monitored and delivered using a ProOx110 controller (Biospherix, Parish, NY). Dams were rotated between hyperoxia and room air every 24 hours to prevent maternal lung injury. After seven days, pups were sacrificed by quick decapitation and lung tissue was snap frozen and stored at −80°C until analyzed.

Protein Isolation, SDS-PAGE & Western Blot

Snap-frozen tissue was thawed in protein lysis buffer (50 mM Tris, pH 7.4; 150 mM NaCl, 10% Triton X-100, 10% NP-40) supplemented with 1% protease inhibitor cocktail (Sigma Aldrich, St. Louis, MO) and 0.1 mM PMSF. Tissue was homogenized, incubated on ice for 30 minutes, and then centrifuged at 10,000 rpm for 15 minutes at 4°C. Supernatants were collected and protein concentration was determined by BCA (Thermo Fisher Scientific, Waltham, MA). Samples were diluted in 2xLaemmli's buffer, separated on 15% SDS-PAGE gels, and proteins were transferred to PVDF membranes using Bio-Rad Trans-Blot Turbo Transfer System (Hercules, CA). Membranes were blocked in 5% milk for one hour and then probed with anti-thioredoxin-1 (Cell Signaling, Danvers, MA), anti-flag (Sigma Aldrich), anti-thioredoxin reductase-1 (Abcam, Cambridge, MA) or anti-actin (Sigma Aldrich) primary antibodies overnight at 4°C. Membranes were washed 3 times in TBS/Tween-20 for 5 minutes each then incubated with HRP-conjugated goat anti-rabbit or -mouse (Southern Biotech, Birmingham, AL) secondary antibodies for 1 hour. Bands were detected by chemiluminescence and images were captured on a UVP bioimaging system (Upland, CA).

Immunohistochemistry

Tissues were fixed in 10% neutral buffered formalin and processed on a Leica 300 ASP tissue processor. The paraffin embedded tissues were sectioned at 5 μm. The BenchMark® XT automated slide staining system (Ventana Medical Systems, Inc., Tucson, AZ) was used for the antibody optimization and staining. The Ventana iView DAB detection kit was used as the chromogen and the slides were counterstained with hematoxylin. Omission of the primary antibody served as the negative control. Anti-thioredoxin-1 primary antibody (Cell Signaling) was used at a dilution of 1:200.

Recombinant Protein Expression

hTrx1 wild-type, $hTrx1^{C32S}$, $hTrx1^{C35S}$, and $hTrx1^{C32,35S}$ sequences were cloned into the pGEX-2TK-GST plasmid (GE Healthcare, Little Chalfont, United Kingdom) and transformed into BL21(DE3)pLysS E. coli. The cells were grown in 2xYTA medium (yeast extract, tryptone, NaCl, 100 ug/mL ampicillin) and expression of the GST-tagged hTrx proteins was induced with 0.1 mM isopropyl-beta-D-thiogalactopyranoside (IPTG) (Thermo Scientific). After four hours incubation with IPTG, the bacteria were pelleted by centrifugation for 10 minutes at 4°C at 7700×g. Once the supernatant was removed, the bacterial cell pellet was lysed with 4 mL BPER Bacterial Protein Reagent (Thermo Scientific) per gram of cell pellet supplemented with lysozyme, DNAse 1, EDTA-free protease inhibitors, and PMSF. The sample was incubated for 15 minutes at room temperature, and then spun at 15,000×g for 15 minutes at 4°C. The supernatant was then purified using a GST Spin Purification Kit (Pierce) according to the manufacturer's directions. Elution of the hTrx1 proteins was done by thrombin cleavage. After the addition of the supernatant to the column and the washing steps, columns were incubated overnight in thrombin cleavage buffer (100 U Thrombin; MP Biomedicals, Santa Ana, CA) in phosphate buffered saline. Recombinant hTrx1 proteins were then eluted with the elution buffer from the purification kit and desalted using Zeba Spin Desalting columns (Thermo Scientific). Total protein concentration was determined by BCA. For Trx1 activity assays, lysates were diluted in activity assay buffer (see below) for input directly into the assay. For Western blot, lysates were diluted in Laemmle's buffer prior to loading on SDS-PAGE gels.

Trx1/TrxR1 Activity Assay

Activities of thioredoxin-1 and thioredoxin reductase-1 were measured using a standard insulin reduction assay (IMCO, Stockholm, Sweden). Snap-frozen tissue was thawed in activity assay buffer (1 mM $NaHPO_4$ anhydrous, 5 mM EDTA pH 8.0) supplemented with 1% protease inhibitor cocktail (Sigma Aldrich), 1% phosphatase inhibitor cocktails 2 and 3 (Sigma Aldrich) and 0.1 mM PMSF. Tissues were homogenized, incubated for 30 minutes on ice and then spun at 10,000 rpm for 15 minutes at 4°C. Supernatants were collected and protein concentration was determined by BCA. Trx1 and TrxR1 activity was analyzed according to the manufacturer's directions.

GSH:GSSG Measurements

Sample derivatization for HPLC was performed as described previously by Jones [24] and modified by Harris and Hansen [25]. Briefly, lung tissue was snap frozen in 5% perchloric

acid supplemented with 10 μM gamma-glutamylglutamate. Once thawed, tissue was ultrasonicated then centrifuged at 14000 g for 10 minutes. The supernatant was set aside and the pellet was solubilized in 100 mM sodium hydroxide. Protein concentration was determined by BCA assay. Iodoacetic acid (14.8 mg/mL) was added to the supernatant to block free thiols, the pH was adjusted to 9.0 with saturated potassium tetraborate, and incubated for 20 minutes. Amino groups were labels with dansyl chloride (20 mg/mL) and the lung lysates were incubated at room temperature in the dark overnight. Derivatization was completed by adding 500 μL chloroform followed by vortexing and centrifugation. GSH and GSSG concentrations were resolved and quantified using reverse-phase HPLC (Waters 2695 Alliance Separations Module with a Supelcosil LC-NH_2 column). Detection of peaks was made using a Waters 2474 fluorescence detector (335 nm/518 nm). Molarity values of GSH and GSSG were determined through standardization with the internal standard (gamma-glutamylglutamate) and sample protein concentrations. Redox potentials were calculated using the Nernst equation [26].

Immunoprecipitation and Mass Spectrometry

Frozen lung tissue was thawed in non-denaturing IP-Lysis Buffer (1 M Tris HCl pH7.4, 5 M NaCl, 0.5 mM EDTA pH 8.0, 1% protease inhibitor, phosphatase inhibitor cocktails 2 and 3, 0.1 mM PMSF, 5 mM iodoacetic acid). Tissue was homogenized, incubated at 4°C on a rotator for 2 hours, and then centrifuged at 12,000 rpm for 20 minutes at 4°C. Supernatants were collected and protein concentration was determined by BCA. 800 μg of lung lysate was added to 50 μL of anti-flag M2 magnetic beads (Sigma Aldrich). The sample:bead mixture was rotated overnight at 4°C. After washing five times with 1×TBS, proteins were eluted from the beads in 50 μL 2xLaemlli's buffer (Biorad) by boiling. Lung eluates were pooled by eluting into the same 50 μL of 2xLaemlli's. 40 μL of the eluate was run on a Mini-PROTEAN TGX gradient (8–16%) precast gel (Biorad, Hercules, CA) and bands were detected by silver stain for mass spectrometry (Thermo Fisher Scientific). IgG bands were excised and the gels were destained according to the manufacturer's directions. Samples were analyzed by LC-MS/MS using a LTQ Orbitrap Velos mass spectrometer (Thermo Fisher Scientific). Peptides were analyzed using Sequest (Thermo Fisher Scientific; version 1.3.0.339). Sequest was set up to search assuming the digestion enzyme trypsin. Sequest was searched with a fragment ion mass tolerance of 0.80 Da and a parent ion tolerance of 10.0 PPM. Oxidation of methionine and carbamidomethyl of cysteine were specified in Sequest as variable modifications. Scaffold (version Scaffold_4.4.6, Proteome Software Inc., Portland, OR) was used to validate MS/MS based peptide and protein identifications. Peptide identifications were accepted if they could be established at greater than 12.0% probability to achieve a false discovery rate (FDR) less than 0.1% by the Scaffold Local FDR algorithm. Protein identifications were accepted if they (i) could be established at greater than 99.0% probability, (ii) contained at least 2 unique peptides, and (iii) were not detected in control samples. Protein probabilities were assigned by the Protein Prophet algorithm [27]. Proteins that contained similar peptides and could not be differentiated based on MS/MS analysis alone were grouped to satisfy the principles of parsimony. Proteins sharing significant peptide evidence were grouped into clusters. Mass spectrometry data was visualized in Scaffold 4 and highlighted results were chosen based on unique peptides found only in the samples from the thioredoxin substrate mouse.

Statistical Analyses

Values represent mean ± standard deviation of biological replicates. The Student's t-test was used to determine significance using GraphPad Prism 5 (GraphPad Software, La Jolla, CA). Statistical significance was defined as $p \leq 0.05$.

RESULTS

Cre-inducible expression of flag-hTrx1^{C35S}

The flag-hTrx1^{C35S} gene was successfully inserted into the genome of the Rosa26-3attP founder (Figure 2A). Both the CAG-promoter and the poly-A tail portion of the transgene were detected by PCR (Figure 2B). The inclusion of the loxP-stop-loxP sequence was incorporated into the flag-hTrx1^{C35S} mice for spatial and temporal regulation of the substrate trap. Mouse embryonic fibroblasts derived from flag-hTrx1^{C35S} mice displayed dose-dependent expression of the transgene through induction with recombinant tat-cre (data not shown). For this study, we obtained global expression of the transgene in all tissues by generating the actin-cre;flag-hTrx1^{C35S} mice with ubiquitous expression of cre recombinase (Figure 3A). Expression of flag-hTrx1^{C35S} was only observed in actin-cre;flag-hTrx1^{C35S} tissues and not the actin-cre controls (Figure 3B). This was evidenced by the hTrx1 doublet as the flag epitope adds approximately 6 kDa to hTrx1. Expression of flag-hTrx1^{C35S} did not alter the levels of endogenous mouse Trx1 or its corresponding reductase, TrxR1 (Figure 3B). The expression pattern of the flag-hTrx1^{C35S} was corroborated in the major tissues using immunochemistry (Figure 3C). Unlike in the actin-cre controls which have defined, localized expression of endogenous Trx1, actin-cre;flag-hTrx1^{C35S} mice had robust transgene expression in brain, lung, heart, liver, and kidney. Taken together, these results illustrate that flag-hTrx^{C35S} was successfully expressed in viable offspring.

hTrx1^{C35S} expression does not disrupt endogenous thioredoxin and glutathione systems. Recent work has indicated that overexpression of mutant hTrx1 in mice effects the expression of the endogenous mouse Trx1. Constitutive overexpression of a catalytic-dead hTrx1 mutant severely inhibited endogenous Trx1 activity in mice [28]. Although expression of flag-hTrx1^{C35S} did not affect expression of endogenous Trx1 (Figure 3B), we tested if the substrate trap transgene exerted dominant-negative effects on endogenous Trx1 activity. First, we measured the activity of several recombinant hTrx1 mutations to demonstrate that the C35S mutation did not exhibit oxidoreductase activity. Recombinant hTrx1 wild-type as well as hTrx1^{C32S}, hTrx1^{C35S}, and hTrx1^{C32,35S} were generated using a bacterial expression system (Figure 4A). Wild-type Trx1 had a dose-dependent increase in Trx activity (Figure 4B). Mutation of either the attacking (C32S) or resolving (C35S) cysteine abolished activity (Figure 4B). This confirms that hTrx1^{C35S} does not display any oxidoreductase activity.

Second, we collected samples from actin-cre;flag-hTrx1^{C35S} mice for Trx1 activity assays. In these mice, the activity of endogenous Trx1 and its reductase, TrxR1, was unchanged compared to actin-cre control mice (Figure 5A,B). It was also important to determine if expression of flag-hTrx1^{C35S} had any effects on the glutathione system which is also responsible for cellular redox homeostasis. While there was slight but not significant oxidation of glutathione (GSSG) in the liver, there was no measurable oxidation of

glutathione in all other tissues (Figure 5C,D). Furthermore, flag-hTrx1^{C35S} expression did not alter glutathione redox potential (GSH/GSSG E_h) (Figure 5E). These data demonstrate that flag-hTrx1^{C35S} transgene expression does not affect endogenous redox circuitry systems.

Identification of Trx1 disulfide targets in vivo

Immunoprecipitation experiments were performed using lung tissue collected from actin-cre; flag-hTrx1^{C35S} mice and actin-cre controls. To identify Trx1 interactions occurring in lung under homeostatic conditions, immunoprecipitations were performed with eight mouse tissues (four per group). The four eluate samples were pooled by boiling, in succession, in the same Laemmli's buffer. This strategy was used in order to ensure equal contributions from multiple mice as well as to minimize sample-sample variations and detection of false-positives. For hyperoxia-induced interactions, mice were maintained in 85% oxygen for the first seven days of life and lung tissues were treated in the same manner. Flag-hTrx1^{C35S}:substrate complexes were captured using paramagnetic beads conjugated to anti-flag antibodies. The input sample (unprocessed lung lysate), as well as the eluate, which was collected by boiling the beads in Laemmli's buffer, were separated by SDS-PAGE and subjected to silver stain (Figure 6A). The expression and purification of flag-hTrx1^{C35S} was detected in actin-cre;flag-hTrx1^{C35S} lung eluates via Western blot, both with anti-Trx1 and anti-flag antibodies (Figure 6B,C). For the gels which were silver stained, the eluate samples were collected for mass spectrometry (Figure 6A).

Mass spectrometry identified 41 static interactions and 17 hyperoxia-induced interactions of Trx1 (Tables 1 and 2). For the homeostatic interactions, the flag-hTrx1^{C35S} transgene and several known Trx1 substrates, peroxiredoxin 1 (Prxn1), peroxiredoxin 5 (Prxn5), peroxiredoxin 2 (Prxn2) and collapsin response mediator protein 2 (Crmp2) were present. Actin-cre;flag-hTrx1^{C35S} mice, and corresponding littermate controls, were challenged using a well characterized oxygen exposure model which recapitulates the premature infant lung disease bronchopulmonary dysplasia [29]. It has been previously shown that hyperoxia treatment in mice oxidizes Trx1, but does not change its expression [30]. Alterations of Trx1 activity as well as expression have been associated with oxygen-induced pathologies, including bronchopulmonary dysplasia (BPD) and asthma [31]. In response to hyperoxia, several new oxygen-dependent Trx1 interactions were detected (Table 2). Of particular interest are several cytoskeleton interacting proteins including capping protein (actin filament) muscle Z-line, beta, isoform CRA (Capzb), band 3 anion transport protein (alc4a1) carbonic anhydrase 2 (CA2), guanine nucleotide-binding protein subunits beta-2-like1 (Gnb1l1), and tubulin beta-4B chain (Tubb4b) because of their possible involvement in alveolar development and injury. These data establish the functionality of the Trx1 substrate trap in vivo and demonstrate how this approach can be used to identify redox-dependent Trx1 signaling pathways in the pathogenesis of oxidative diseases.

DISCUSSION

Reversible oxidation of thiol switches is a mechanism to regulate activities of non-redox proteins. This notion has been supported by (i) cysteine conservation across organisms, (ii)

high cysteine reactivity under biological conditions, (iii) and frequent location of cysteines adjacent to functional sites [32–34]. Oxidation and reduction of cysteines creates a mechanism by which protein activity can be controlled through activities of cysteine-recognizing redox enzymes. This group of proteins includes the thioredoxin- and glutathione-dependent enzyme systems. In addition to serving an antioxidant capacity, Trx1 has been recognized as an important regulator of thiol switches and plays a direct role in controlling intracellular and extracellular signaling, regulation of gene expression, growth and proliferation, and metabolism [31]. Trx1 also functions to control protein folding [35], denitrosylation [36], and reduction of sulfhydration and sulfenic acid [37, 38]. Trx1 regulation of cysteine redox status is an important mechanism to promote sensing and adaptation environmental oxidants via the activities of thiol switches.

A technical challenge when identifying functional thiol switches is the rapid nature by which redox reactions occur. ICAT with addition of HPDP-biotin has been instrumental in identifying Trx1-dependent denitrosylation of substrates [39]. In a neuroblastoma cell line, ICAT was successfully used to identify peroxiredoxin 1 (Prxn1), cyclophilin A, and cofilin-1, as well as several ribosomal proteins and elongation factors, whose nitrosylation status is controlled by Trx1 [9]. Samples derived from mouse cardiac tissue, have identified several Trx1 targets, including metabolic enzymes such as glyceraldehyde-3-phosphate dehydrogenase and fatty acid-binding protein [10]. The major drawback to the ICAT technique is that it only measures indirect Trx1 interactions in sample lysates. Unlike the ICAT method, the thioredoxin substrate trap assesses direct Trx1 interactions in intact biological systems. Endogenous expression of a Trx1 protein where the Cys35 residue is mutated to serine creates a stable intermediate between thioredoxin and its substrate and these complexes are then analyzed with mass spectrometry. We have successfully used this technique for proteomic identification of novel Trx1 substrates in lung adenocarcinoma cells [17]. We have taken this method one step further and created a novel transgenic mouse model that expresses the Trx1 substrate trap. With this model, we have identified known and novel static and hyperoxia-induced interactions of Trx1 which are potential thiol switches in vivo.

Homeostatic Trx1 Interactions

We identified several known and novel Trx1 substrates in lungs of actin-cre;flag-hTrx1^{C35S} mice. Of the five members of the peroxiredoxin family known to interact with Trx1, Prxn1, Prxn2, and Prxn5 were identified by mass spectrometry. Peroxiredoxins and thioredoxins are known to coordinate oxidation and reduction of thiol switches respectively. For example, Prxn2 was recently shown to transmit oxidizing equivalents of hydrogen peroxide to STAT3 which is then reduced by Trx1 [40]. We also identified 14-3-3 protein theta and 40S ribosomal protein 11 which have been show to interact with Trx1 [9, 41]. Of particular interest is a known target of Trx1 that was determined by mass spectrometry, collapsin response mediator protein 2 (Crmp2). Crmp2 has five phosphorylation sites (Tyr479, Thr509/514/555, Ser522), as well as undergoes SUMOylation at Lys374 and reversible oxidation at Cys504, all of which have been shown to alter the function of this protein [42–44]. Interestingly, all the aforementioned posttranslational modifications reside in the same region of the protein, suggesting a correlation between redox, phosphorylation, and

SUMOylation modifications in the regulation of Crmp2 function. For example, the oxidation status of Cys504 defines two conformations of the Crmp2 complex and accumulation of oxidized Crmp2 correlates with neurite outgrowth [45]. Crmp2 reduction leads to the more open Crmp2 complex conformation with greater exposure of hydrophobic regions which interact with subsequent effector molecules such as kinases or phosphatases [45]. Interestingly, the Trx1:Crmp2 interaction was mapped to the Cys504 residue of Crmp2, suggesting that Trx1 is an important determinant of Crmp2 posttranslational modifications and function [46]. Although Crmp2 has been primarily associated with neurological diseases including Alzheimer's and schizophrenia [47–50], Crmp2 is highly expressed in lung tissue as well as lung tumor cells [51]. Although endogenous function of Crmp2 in the lung remains unknown, differential Crmp2 posttranslational modifications are associated with nonsmall cell lung cancer [52]. The detection of known Trx1 substrates in this transgenic mouse model demonstrates the functionality of our Trx1 substrate trap mouse and our results are the first evidence that Trx1 interacts with Crmp2 in the lung in vivo.

We also identified several novel substrates of Trx1 which have direct relevance to lung function and disease: collapsin response mediator protein 4 (Crmp4), cysteine and glycine rich protein 1 (Csrp1), protein Tns 1 (Tns1), and leukocyte elastase inhibitor A (Serpinb1a). Crmp4 has high association with lung [53] cancers. Csrp1 may play a role in lung fibrosis [54]. Several genome wide association studies have identified Tns1 as an important determinant of lung function [55] and have linked this protein to an increased risk for COPD [56] as well as allergy associated asthma [57]. Serpinb1a is a serine protease inhibitor which is secreted into the bronchoalveolar space and has been associated with cystic fibrosis [58], chronic lung disease of prematurity [59] and sarcoidosis [60]. It is important to note that the results described here are from total lung lysates and the role of cell-specific Trx1 interactions is not known.

While we did find known interactions of Trx1, such as peroxiredoxins, we did not find others such as actin. We believe this could be due to the expression level of the transgene as well as to the innate variability of immunoprecipitation experiments. As expected, we did not find TrxR1 because the Trx1 substrate trap cannot form the necessary intramolecular disulfide bond targeted for reduction by TrxR1 [61]. Collectively, these results indicate that the substrate trap is working as expected in our model.

Hyperoxia-Sensitive Trx1 Interactions

Changes in atmospheric oxygen tension can lead to alterations in cellular morphology and organ development. For example, as seen with mechanical ventilation of premature newborns [62] and in animal models of bronchopulmonary dysplasia (BPD) [29, 63], excess oxygen disrupts lung development and function. In this study, we have used a well-established neonatal mouse model of hyperoxia [64] to identify Trx1 substrates under hyperoxic conditions. High oxygen exposure affects lung development and promotes injury in two critical ways: by increasing oxidative stress and altering the cytoskeleton structure. The prevailing hypothesis of hyperoxia-induced lung injury is that excess oxygen promotes the accumulation of reactive oxygen species and causes oxidation of proteins in several cell survival pathways, which leads to cell death [65, 66]. Our previous work has shown that

Trx1 is important for cell survival during hyperoxia [17]. It is well documented that Trx1 translocates to the nucleus during oxidative injury [67] which illustrates the importance of Trx1 in nuclear redox homeostasis. Therefore, it is not surprising that our data showed novel targets of Trx1 that lie in the nucleus, including ATP-dependent RNA helicase DDX3X (Ddx3x), guanine nucleotide-binding protein subunit beta-2-like-1 (Gnb2l1), heterogeneous nuclear ribonuclear protein A3, and 40S ribosomal protein S3a (Rps3a). Studies have shown that hyperoxia causes Trx1 oxidation [17, 68]. This data indicates that the reactive Cys32 of the flag-hTrx1^{C35S} under high oxygen conditions could be oxidized, which may explain why fewer targets of Trx1 were identified in this cohort.

The cytoskeleton is dynamic and responds to multiple cellular stresses. This structure includes the actin-based cytoskeleton and the tubulin-based myotubules. The flexibility of the cytoskeleton in the lung is necessary for alveolar stretch during respiration [69]. Previous studies have shown that the cytoskeleton is altered in hyperoxic conditions. In particular, excess oxygen stimulates the formation of f-actin, which forms disorganized stress fibers throughout the cell body [70, 71]. Trx1 has been shown to interact with actin and inhibit the formation of stress fibers in response to the oxidant hydrogen peroxide [72, 73]. We identified capping protein (actin filament) muscle, Z-line, beta, isoform CRA (Capzb), a protein that is responsible for capping the barbed end of actin filaments as a possible target of Trx1 [74]. The presence of this capping protein prevents the formation of f-actin, and therefore maintains the pool of g-actin, until f-actin formation is desired. Contact with Capzb may be a secondary way Trx1 can control the formation of f-actin fibers during stress. We also identified two myotubule associated proteins, alpha-centractin (Actr1a) and tubulin beta-4B chain (Tubb4b). Tubb4b has a cysteine, Cys12, which is modified by bis(4-fluorbenzyl)trisulfide indicating that it this cysteine could potentially be modified by redox enzymes such as Trx1 [75]. Actr1a is part of the dynactin subunit that has high homology to actin, a known target of Trx1 [76, 77]. Since Trx1 has been shown to be highly involved in cytoskeleton dynamics, we hypothesize that these targets are important in the structural changes induced by hyperoxia.

Conclusions

Here we introduce a novel mouse model to study the interactions of Trx1. This transgenic mouse has conditional expression of a Trx1 substrate trap which stabilizes substrate interactions in vivo which we used for proteomic studies. We identified 41 static and 17 hyperoxic-specific Trx1 interactions in postnatal lung. This is the first study, to our knowledge, to use a direct method to detect and identify Trx1 substrates in vivo. In combination with cell-specific cre drivers, this transgenic mouse is a versatile tool to elucidate Trx1 interactions in vivo and understand the physiological role of redox-dependent Trx1 regulation of thiol switches.

Acknowledgments

This work is supported by the National Institutes of Health (grant number P20 GM103620). Tissue processing and immunohistology was performed with assistance from the Molecular Pathology Core at Sanford Research which is supported by the National Institutes of Health (grant numbers P20 GM103620, P20 GM103548). Mass spectrometry and proteomics were performed by the Arizona Proteomics Consortium which is supported by the National Institutes of Health (grant numbers P30 ES06694, P30 CA023074, S10 RR028868) and by the BIO5

Institute of the University of Arizona. The Cre Repository at The Jackson Laboratory is supported by the National Institutes of Health (grant number OD077790).

REFERENCES

1. Matsui M, Oshima M, Oshima H, Takaku K, Maruyama T, Yodoi J, Taketo MM. Early embryonic lethality caused by targeted disruption of the mouse thioredoxin gene. Developmental biology. 1996; 178:179–185. [PubMed: 8812119]
2. Tipple TE. The thioredoxin system in neonatal lung disease. Antioxidants & redox signaling. 2014; 21:1916–1925. [PubMed: 24328910]
3. Gromer S, Urig S, Becker K. The thioredoxin system--from science to clinic. Med Res Rev. 2004; 24:40–89. [PubMed: 14595672]
4. Holmgren A, Soderberg BO, Eklund H, Branden CI. Three-dimensional structure of Escherichia coli thioredoxin-S2 to 2.8 A resolution. Proceedings of the National Academy of Sciences of the United States of America. 1975; 72:2305–2309. [PubMed: 1094461]
5. Holmgren A. Thioredoxin structure and mechanism: conformational changes on oxidation of the active-site sulfhydryls to a disulfide. Structure. 1995; 3:239–243. [PubMed: 7788289]
6. Arner ES, Holmgren A. Physiological functions of thioredoxin and thioredoxin reductase. Eur J Biochem. 2000; 267:6102–6109. [PubMed: 11012661]
7. Holmgren A. Thioredoxin and glutaredoxin systems. The Journal of biological chemistry. 1989; 264:13963–13966. [PubMed: 2668278]
8. Hagglund P, Bunkenborg J, Maeda K, Svensson B. Identification of thioredoxin disulfide targets using a quantitative proteomics approach based on isotope-coded affinity tags. J Proteome Res. 2008; 7:5270–5276. [PubMed: 19367707]
9. Wu C, Parrott AM, Liu T, Jain MR, Yang Y, Sadoshima J, Li H. Distinction of thioredoxin transnitrosylation and denitrosylation target proteins by the ICAT quantitative approach. J Proteomics. 2011; 74:2498–2509. [PubMed: 21704743]
10. Fu C, Wu C, Liu T, Ago T, Zhai P, Sadoshima J, Li H. Elucidation of thioredoxin target protein networks in mouse. Mol Cell Proteomics. 2009; 8:1674–1687. [PubMed: 19416943]
11. Wu C, Parrott AM, Fu C, Liu T, Marino SM, Gladyshev VN, Jain MR, Baykal AT, Li Q, Oka S, Sadoshima J, Beuve A, Simmons WJ, Li H. Thioredoxin 1-mediated posttranslational modifications: reduction, transnitrosylation, denitrosylation, and related proteomics methodologies. Antioxidants & redox signaling. 2011; 15:2565–2604. [PubMed: 21453190]
12. Kallis GB, Holmgren A. Differential reactivity of the functional sulfhydryl groups of cysteine-32 and cysteine-35 present in the reduced form of thioredoxin from Escherichia coli. The Journal of biological chemistry. 1980; 255:10261–10265. [PubMed: 7000775]
13. Depuydt M, Leonard SE, Vertommen D, Denoncin K, Morsomme P, Wahni K, Messens J, Carroll KS, Collet JF. A periplasmic reducing system protects single cysteine residues from oxidation. Science. 2009; 326:1109–1111. [PubMed: 19965429]
14. Verdoucq L, Vignols F, Jacquot JP, Chartier Y, Meyer Y. In vivo characterization of a thioredoxin h target protein defines a new peroxiredoxin family. The Journal of biological chemistry. 1999; 274:19714–19722. [PubMed: 10391912]
15. Brandes HK, Larimer FW, Hartman FC. The molecular pathway for the regulation of phosphoribulokinase by thioredoxin f. The Journal of biological chemistry. 1996; 271:3333–3335. [PubMed: 8631927]
16. Brandes HK, Larimer FW, Geck MK, Stringer CD, Schurmann P, Hartman FC. Direct identification of the primary nucleophile of thioredoxin f. The Journal of biological chemistry. 1993; 268:18411–18414. [PubMed: 8395501]
17. Floen MJ, Forred BJ, Bloom EJ, Vitiello PF. Thioredoxin-1 redox signaling regulates cell survival in response to hyperoxia. Free radical biology & medicine. 2014; 75:167–177. [PubMed: 25106706]
18. Wu C, Jain MR, Li Q, Oka S, Li W, Kong AN, Nagarajan N, Sadoshima J, Simmons WJ, Li H. Identification of novel nuclear targets of human thioredoxin 1. Mol Cell Proteomics. 2014; 13:3507–3518. [PubMed: 25231459]

19. Karlenius TC, Tonissen KF. Thioredoxin and Cancer: A Role for Thioredoxin in all States of Tumor Oxygenation. Cancers. 2010; 2:209–232. [PubMed: 24281068]
20. Jorgenson TC, Zhong W, Oberley TD. Redox imbalance and biochemical changes in cancer. Cancer research. 2013; 73:6118–6123. [PubMed: 23878188]
21. Lewandoski M, Meyers EN, Martin GR. Analysis of Fgf8 gene function in vertebrate development. Cold Spring Harbor symposia on quantitative biology. 1997; 62:159–168. [PubMed: 9598348]
22. Liu Y, Min W. Thioredoxin promotes ASK1 ubiquitination and degradation to inhibit ASK1-mediated apoptosis in a redox activity-independent manner. Circ Res. 2002; 90:1259–1266. [PubMed: 12089063]
23. Yee M, Vitiello PF, Roper JM, Staversky RJ, Wright TW, McGrath-Morrow SA, Maniscalco WM, Finkelstein JN, O'Reilly MA. Type II epithelial cells are critical target for hyperoxia-mediated impairment of postnatal lung development. American journal of physiology. Lung cellular and molecular physiology. 2006; 291:L1101–L1111. [PubMed: 16861382]
24. Jones DP. Redox potential of GSH/GSSG couple: assay and biological significance. Methods Enzymol. 2002; 348:93–112. [PubMed: 11885298]
25. Harris C, Hansen JM. Oxidative stress, thiols, and redox profiles. Methods in molecular biology. 2012; 889:325–346. [PubMed: 22669675]
26. Harris C, Shuster DZ, Roman Gomez R, Sant KE, Reed MS, Pohl J, Hansen JM. Inhibition of glutathione biosynthesis alters compartmental redox status and the thiol proteome in organogenesis-stage rat conceptuses. Free radical biology & medicine. 2013; 63:325–337. [PubMed: 23736079]
27. Nesvizhskii AI, Keller A, Kolker E, Aebersold R. A statistical model for identifying proteins by tandem mass spectrometry. Anal Chem. 2003; 75:4646–4658. [PubMed: 14632076]
28. Das KC. Thioredoxin-deficient mice, a novel phenotype sensitive to ambient air and hypersensitive to hyperoxia-induced lung injury. American journal of physiology. Lung cellular and molecular physiology. 2015; 308:L429–L442. [PubMed: 25539854]
29. Berger J, Bhandari V. Animal Models of Bronchopulmonary Dysplasia. I: The Term Mouse Models. American journal of physiology. Lung cellular and molecular physiology ajplung. 2014; 00159:2014.
30. Tipple TE, Welty SE, Rogers LK, Hansen TN, Choi YE, Kehrer JP, Smith CV. Thioredoxin-related mechanisms in hyperoxic lung injury in mice. American journal of respiratory cell and molecular biology. 2007; 37:405–413. [PubMed: 17575077]
31. Lillig CH, Holmgren A. Thioredoxin and related molecules--from biology to health and disease. Antioxidants & redox signaling. 2007; 9:25–47. [PubMed: 17115886]
32. Deponte M, Lillig CH. Enzymatic control of cysteinyl thiol switches in proteins. Biol Chem. 2015; 396:401–413. [PubMed: 25581754]
33. Marino SM, Gladyshev VN. Cysteine function governs its conservation and degeneration and restricts its utilization on protein surfaces. Journal of molecular biology. 2010; 404:902–916. [PubMed: 20950627]
34. Ondrechen MJ, Clifton JG, Ringe D. THEMATICS: a simple computational predictor of enzyme function from structure. Proceedings of the National Academy of Sciences of the United States of America. 2001; 98:12473–12478. [PubMed: 11606719]
35. Holmgren A. Thioredoxin. Annu Rev Biochem. 1985; 54:237–271. [PubMed: 3896121]
36. Benhar M, Thompson JW, Moseley MA, Stamler JS. Identification of S-nitrosylated targets of thioredoxin using a quantitative proteomic approach. Biochemistry. 2010; 49:6963–6969. [PubMed: 20695533]
37. Krishnan N, Fu C, Pappin DJ, Tonks NK. H2S-Induced sulfhydration of the phosphatase PTP1B and its role in the endoplasmic reticulum stress response. Sci Signal. 2011; 4:ra86. [PubMed: 22169477]
38. Nelson KJ, Klomsiri C, Codreanu SG, Soito L, Liebler DC, Rogers LC, Daniel LW, Poole LB. Use of dimedone-based chemical probes for sulfenic acid detection methods to visualize and identify labeled proteins. Methods Enzymol. 2010; 473:95–115. [PubMed: 20513473]
39. Wu C, Parrott AM, Liu T, Beuve A, Li H. Functional proteomics approaches for the identification of transnitrosylase and denitrosylase targets. Methods. 2013; 62:151–160. [PubMed: 23428400]

40. Sobotta MC, Liou W, Stocker S, Talwar D, Oehler M, Ruppert T, Scharf AN, Dick TP. Peroxiredoxin-2 and STAT3 form a redox relay for H2O2 signaling. Nature chemical biology. 2015; 11:64–70. [PubMed: 25402766]
41. Meek SE, Lane WS, Piwnica-Worms H. Comprehensive proteomic analysis of interphase and mitotic 14-3-3-binding proteins. The Journal of biological chemistry. 2004; 279:32046–32054. [PubMed: 15161933]
42. Yoshimura T, Kawano Y, Arimura N, Kawabata S, Kikuchi A, Kaibuchi K. GSK-3beta regulates phosphorylation of CRMP-2 and neuronal polarity. Cell. 2005; 120:137–149. [PubMed: 15652488]
43. Arimura N, Menager C, Kawano Y, Yoshimura T, Kawabata S, Hattori A, Fukata Y, Amano M, Goshima Y, Inagaki M, Morone N, Usukura J, Kaibuchi K. Phosphorylation by Rho kinase regulates CRMP-2 activity in growth cones. Molecular and cellular biology. 2005; 25:9973–9984. [PubMed: 16260611]
44. Arimura N, Inagaki N, Chihara K, Menager C, Nakamura N, Amano M, Iwamatsu A, Goshima Y, Kaibuchi K. Phosphorylation of collapsin response mediator protein-2 by Rho-kinase. Evidence for two separate signaling pathways for growth cone collapse. J. Biol. Chem. 2000; 275:23973–23980. [PubMed: 10818093]
45. Gellert M, Venz S, Mitlohner J, Cott C, Hanschmann EM, Lillig CH. Identification of a dithiol-disulfide switch in collapsin response mediator protein 2 (CRMP2) that is toggled in a model of neuronal differentiation. The Journal of biological chemistry. 2013; 288:35117–35125. [PubMed: 24133216]
46. Morinaka A, Yamada M, Itofusa R, Funato Y, Yoshimura Y, Nakamura F, Yoshimura T, Kaibuchi K, Goshima Y, Hoshino M, Kamiguchi H, Miki H. Thioredoxin mediates oxidation-dependent phosphorylation of CRMP2 and growth cone collapse. Sci Signal. 2011; 4:ra26. [PubMed: 21521879]
47. Williamson R, van Aalten L, Mann DM, Platt B, Plattner F, Bedford L, Mayer J, Howlett D, Usardi A, Sutherland C, Cole AR. CRMP2 hyperphosphorylation is characteristic of Alzheimer's disease and not a feature common to other neurodegenerative diseases. J Alzheimers Dis. 2011; 27:615–625. [PubMed: 21860090]
48. Silva PN, Furuya TK, Sampaio Braga I, Rasmussen LT, de Labio RW, Bertolucci PH, Chen ES, Turecki G, Mechawar N, Payao SL, Mill J, Smith MC. CNP and DPYSL2 mRNA expression and promoter methylation levels in brain of Alzheimer's disease patients. J Alzheimers Dis. 2013; 33:349–355. [PubMed: 22954668]
49. Liu Y, Pham X, Zhang L, Chen PL, Burzynski G, McGaughey DM, He S, McGrath JA, Wolyniec P, Fallin MD, Pierce MS, McCallion AS, Pulver AE, Avramopoulos D, Valle D. Functional variants in DPYSL2 sequence increase risk of schizophrenia and suggest a link to mTOR signaling. G3 (Bethesda). 2014; 5:61–72. [PubMed: 25416705]
50. Lee H, Joo J, Nah SS, Kim JW, Kim HK, Kwon JT, Lee HY, Kim YO, Kim HJ. Changes in Dpysl2 expression are associated with prenatally stressed rat offspring and susceptibility to schizophrenia in humans. Int J Mol Med. 2015; 35:1574–1586. [PubMed: 25847191]
51. Uhlen M, Fagerberg L, Hallstrom BM, Lindskog C, Oksvold P, Mardinoglu A, Sivertsson A, Kampf C, Sjostedt E, Asplund A, Olsson I, Edlund K, Lundberg E, Navani S, Szigyarto CA, Odeberg J, Djureinovic D, Takanen JO, Hober S, Alm T, Edqvist PH, Berling H, Tegel H, Mulder J, Rockberg J, Nilsson P, Schwenk JM, Hamsten M, von Feilitzen K, Forsberg M, Persson L, Johansson F, Zwahlen M, von Heijne G, Nielsen J, Ponten F. Proteomics. Tissue-based map of the human proteome. Science. 2015; 347:1260419. [PubMed: 25613900]
52. Oliemuller E, Pelaez R, Garasa S, Pajares MJ, Agorreta J, Pio R, Montuenga LM, Teijeira A, Llanos S, Rouzaut A. Phosphorylated tubulin adaptor protein CRMP-2 as prognostic marker and candidate therapeutic target for NSCLC. International journal of cancer. Journal international du cancer. 2013; 132:1986–1995. [PubMed: 23023514]
53. Okita K, Motohashi S, Shinnakasu R, Nagato K, Yamasaki K, Sato Y, Kitamura H, Hijikata A, Yamashita M, Shimizu K, Fujii S, Ohara O, Taniguchi M, Sakaida I, Nakayama T. A set of genes associated with the interferon-gamma response of lung cancer patients undergoing alpha-galactosylceramide-pulsed dendritic cell therapy. Cancer Sci. 2010; 101:2333–2340. [PubMed: 20804502]

54. Jarvinen PM, Myllarniemi M, Liu H, Moore HM, Lepparanta O, Salmenkivi K, Koli K, Latonen L, Band AM, Laiho M. Cysteine-rich protein 1 is regulated by transforming growth factor-beta1 and expressed in lung fibrosis. J Cell Physiol. 2012; 227:2605–2612. [PubMed: 21882188]

55. Repapi E, Sayers I, Wain LV, Burton PR, Johnson T, Obeidat M, Zhao JH, Ramasamy A, Zhai G, Vitart V, Huffman JE, Igl W, Albrecht E, Deloukas P, Henderson J, Granell R, McArdle WL, Rudnicka AR, Wellcome Trust Case Control, C. Barroso I, Loos RJ, Wareham NJ, Mustelin L, Rantanen T, Surakka I, Imboden M, Wichmann HE, Grkovic I, Jankovic S, Zgaga L, Hartikainen AL, Peltonen L, Gyllensten U, Johansson A, Zaboli G, Campbell H, Wild SH, Wilson JF, Glaser S, Homuth G, Volzke H, Mangino M, Soranzo N, Spector TD, Polasek O, Rudan I, Wright AF, Heliovaara M, Ripatti S, Pouta A, Naluai AT, Olin AC, Toren K, Cooper MN, James AL, Palmer LJ, Hingorani AD, Wannamethee SG, Whincup PH, Smith GD, Ebrahim S, McKeever TM, Pavord ID, MacLeod AK, Morris AD, Porteous DJ, Cooper C, Dennison E, Shaheen S, Karrasch S, Schnabel E, Schulz H, Grallert H, Bouatia-Naji N, Delplanque J, Froguel P, Blakey JD, Team NRS, Britton JR, Morris RW, Holloway JW, Lawlor DA, Hui J, Nyberg F, Jarvelin MR, Jackson C, Kahonen M, Kaprio J, Probst-Hensch NM, Koch B, Hayward C, Evans DM, Elliott P, Strachan DP, Hall IP, Tobin MD. Genome-wide association study identifies five loci associated with lung function. Nature genetics. 2010; 42:36–44. [PubMed: 20010834]

56. Soler Artigas M, Wain LV, Repapi E, Obeidat M, Sayers I, Burton PR, Johnson T, Zhao JH, Albrecht E, Dominiczak AF, Kerr SM, Smith BH, Cadby G, Hui J, Palmer LJ, Hingorani AD, Wannamethee SG, Whincup PH, Ebrahim S, Smith GD, Barroso I, Loos RJ, Wareham NJ, Cooper C, Dennison E, Shaheen SO, Liu JZ, Marchini J, Medical Research Council National Survey of, H.;Development Respiratory Study, T. Dahgam S, Naluai AT, Olin AC, Karrasch S, Heinrich J, Schulz H, McKeever TM, Pavord ID, Heliovaara M, Ripatti S, Surakka I, Blakey JD, Kahonen M, Britton JR, Nyberg F, Holloway JW, Lawlor DA, Morris RW, James AL, Jackson CM, Hall IP, Tobin MD, SpiroMeta C. Effect of five genetic variants associated with lung function on the risk of chronic obstructive lung disease, and their joint effects on lung function. American journal of respiratory and critical care medicine. 2011; 184:786–795. [PubMed: 21965014]

57. Ferreira MA, Matheson MC, Tang CS, Granell R, Ang W, Hui J, Kiefer AK, Duffy DL, Baltic S, Danoy P, Bui M, Price L, Sly PD, Eriksson N, Madden PA, Abramson MJ, Holt PG, Heath AC, Hunter M, Musk B, Robertson CF, Le Souef P, Montgomery GW, Henderson AJ, Tung JY, Dharmage SC, Brown MA, James A, Thompson PJ, Pennell C, Martin NG, Evans DM, Hinds DA, Hopper JL. Australian Asthma Genetics Consortium, C. Genome-wide association analysis identifies 11 risk variants associated with the asthma with hay fever phenotype. J Allergy Clin Immunol. 2014; 133:1564–1571. [PubMed: 24388013]

58. Cooley J, Sontag MK, Accurso FJ, Remold-O'Donnell E. SerpinB1 in cystic fibrosis airway fluids: quantity, molecular form and mechanism of elastase inhibition. The European respiratory journal. 2011; 37:1083–1090. [PubMed: 20817705]

59. Davies PL, Spiller OB, Beeton ML, Maxwell NC, Remold-O'Donnell E, Kotecha S. Relationship of proteinases and proteinase inhibitors with microbial presence in chronic lung disease of prematurity. Thorax. 2010; 65:246–251. [PubMed: 20335295]

60. Maver A, Medica I, Peterlin B. Search for sarcoidosis candidate genes by integration of data from genomic, transcriptomic and proteomic studies. Med Sci Monit. 2009; 15:SR22–SR28. [PubMed: 19946248]

61. Reichard P. 4th FEBS Meeting's Plenary Lecture. The biosynthesis of deoxyribonucleotides. Eur J Biochem. 1968; 3:259–266. [PubMed: 4385004]

62. Gough A, Linden M, Spence D, Patterson CC, Halliday HL, McGarvey LP. Impaired lung function and health status in adult survivors of bronchopulmonary dysplasia. The European respiratory journal. 2014; 43:808–816. [PubMed: 23900988]

63. Coalson JJ, Kuehl TJ, Escobedo MB, Hilliard JL, Smith F, Meredith K, Null DM Jr, Walsh W, Johnson D, Robotham JL. A baboon model of bronchopulmonary dysplasia. II. Pathologic features. Experimental and molecular pathology. 1982; 37:335–350. [PubMed: 6924896]

64. Bonikos DS, Bensch KG, Ludwin SK, Northway WH Jr. Oxygen toxicity in the newborn. The effect of prolonged 100 per cent O2 exposure on the lungs of newborn mice. Laboratory investigation; a journal of technical methods and pathology. 1975; 32:619–635. [PubMed: 1092910]

65. Buczynski BW, Maduekwe ET, O'Reilly MA. The role of hyperoxia in the pathogenesis of experimental BPD. Seminars in perinatology. 2013; 37:69–78. [PubMed: 23582960]

66. Corvol H, Flamein F, Epaud R, Clement A, Guillot L. Lung alveolar epithelium and interstitial lung disease. Int J Biochem Cell Biol. 2009; 41:1643–1651. [PubMed: 19433305]

67. Schroeder P, Popp R, Wiegand B, Altschmied J, Haendeler J. Nuclear redox-signaling is essential for apoptosis inhibition in endothelial cells--important role for nuclear thioredoxin-1. Arteriosclerosis, thrombosis, and vascular biology. 2007; 27:2325–2331.

68. Tipple TE, Welty SE, Nelin LD, Hansen JM, Rogers LK. Alterations of the thioredoxin system by hyperoxia: implications for alveolar development. American journal of respiratory cell and molecular biology. 2009; 41:612–619. [PubMed: 19244202]

69. Hossain MM, Smith PG, Wu K, Jin JP. Cytoskeletal tension regulates both expression and degradation of h2-calponin in lung alveolar cells. Biochemistry. 2006; 45:15670–15683. [PubMed: 17176089]

70. Phillips PG, Higgins PJ, Malik AB, Tsan MF. Effect of hyperoxia on the cytoarchitecture of cultured endothelial cells. The American journal of pathology. 1988; 132:59–72. [PubMed: 3394802]

71. Roan E, Wilhelm K, Bada A, Makena PS, Gorantla VK, Sinclair SE, Waters CM. Hyperoxia alters the mechanical properties of alveolar epithelial cells. American journal of physiology. Lung cellular and molecular physiology. 2012; 302:L1235–L1241. [PubMed: 22467640]

72. Wang X, Ling S, Zhao D, Sun Q, Li Q, Wu F, Nie J, Qu L, Wang B, Shen X, Bai Y, Li Y, Li Y. Redox regulation of actin by thioredoxin-1 is mediated by the interaction of the proteins via cysteine 62. Antioxidants & redox signaling. 2010; 13:565–573. [PubMed: 20218863]

73. Zschauer TC, Kunze K, Jakob S, Haendeler J, Altschmied J. Oxidative stress-induced degradation of thioredoxin-1 and apoptosis is inhibited by thioredoxin-1-actin interaction in endothelial cells. Arterioscler Thromb Vasc Biol. 2011; 31:650–656. [PubMed: 21212402]

74. DiNubile MJ, Cassimeris L, Joyce M, Zigmond SH. Actin filament barbed-end capping activity in neutrophil lysates: the role of capping protein-beta 2. Mol Biol Cell. 1995; 6:1659–1671. [PubMed: 8590796]

75. Xu W, Xi B, Wu J, An H, Zhu J, Abassi Y, Feinstein SC, Gaylord M, Geng B, Yan H, Fan W, Sui M, Wang X, Xu X. Natural product derivative Bis(4-fluorobenzyl)trisulfide inhibits tumor growth by modification of beta-tubulin at Cys 12 and suppression of microtubule dynamics. Mol Cancer Ther. 2009; 8:3318–3330. [PubMed: 19996274]

76. Clark SW, Meyer DI. Centractin is an actin homologue associated with the centrosome. Nature. 1992; 359:246–250. [PubMed: 1356230]

77. Karki S, Tokito MK, Holzbaur EL. A dynactin subunit with a highly conserved cysteine-rich motif interacts directly with Arp1. The Journal of biological chemistry. 2000; 275:4834–4839. [PubMed: 10671518]

Highlights

- Characterization of a cre-inducible transgenic mouse to identify Trx1 substrates.
- Detection of previously known and novel Trx1 redox-dependent interactions in vivo.
- Dynamic Trx1 substrates that occur in lung during perinatal hyperoxic injury.

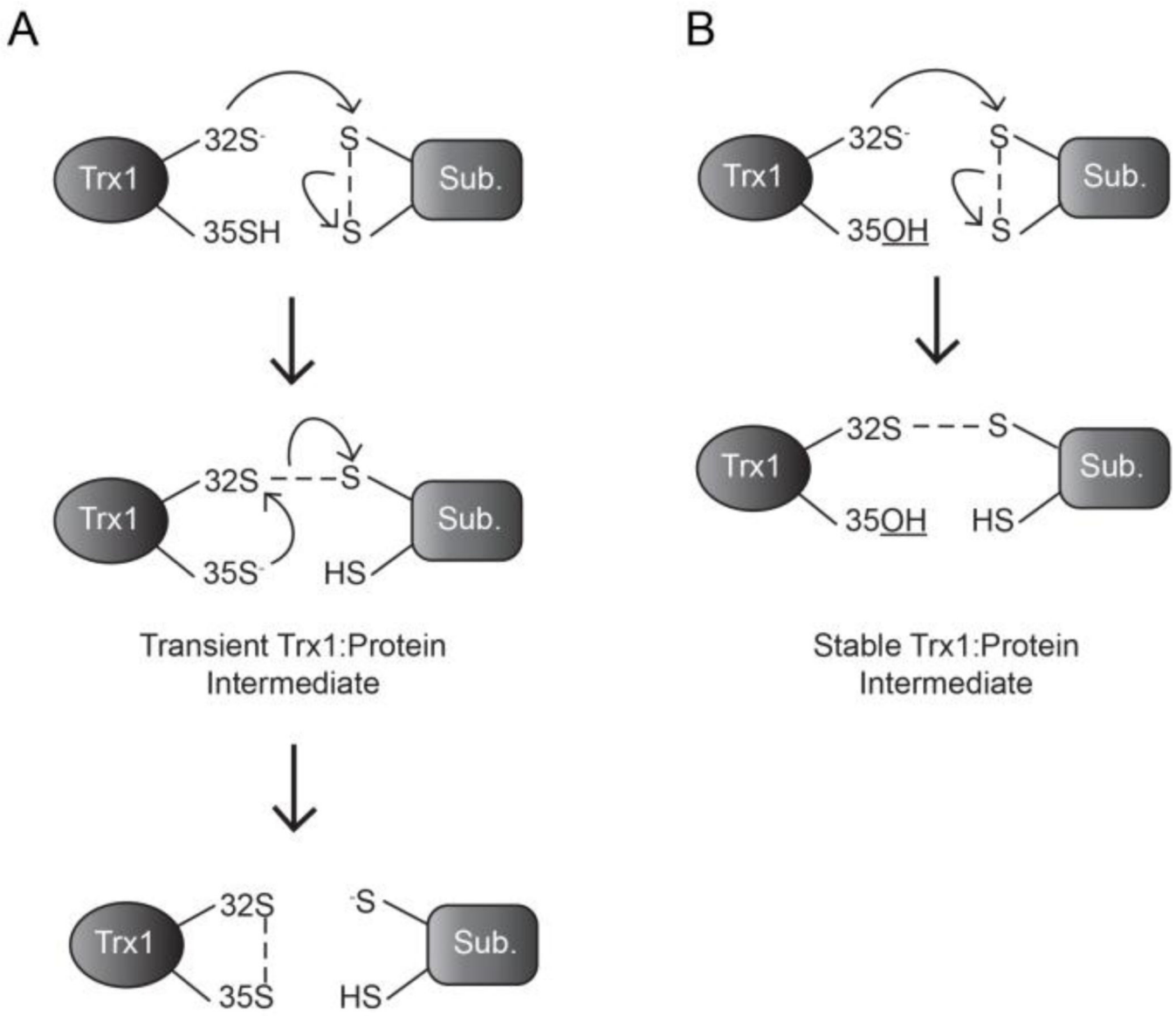

Figure 1.

Mechanism of the hTrx1^{C35S} substrate trap. (A) Mechanism of human Trx1 oxidoreductase function. Nucleophilic attack of the deprotonated Cys32 of Trx1 on the substrate disulfide results in an intermolecular disulfide intermediate. This disulfide intermediate is rapidly attacked by the Cys35 thiolate, releasing the reduced substrate with an intramolecular disulfide in the catalytic site of Trx1. (B) Mutating the resolving Cys35 to serine causes incomplete catalytic activity of Trx1 with the substrate and stabilizes the intermolecular disulfide. Following flag immunoprecipitation of the Trx1:substrate complex, the complexes are boiled off the beads into Laemmli's buffer for subsequent identification via mass spectrometry (Sub = substrate).

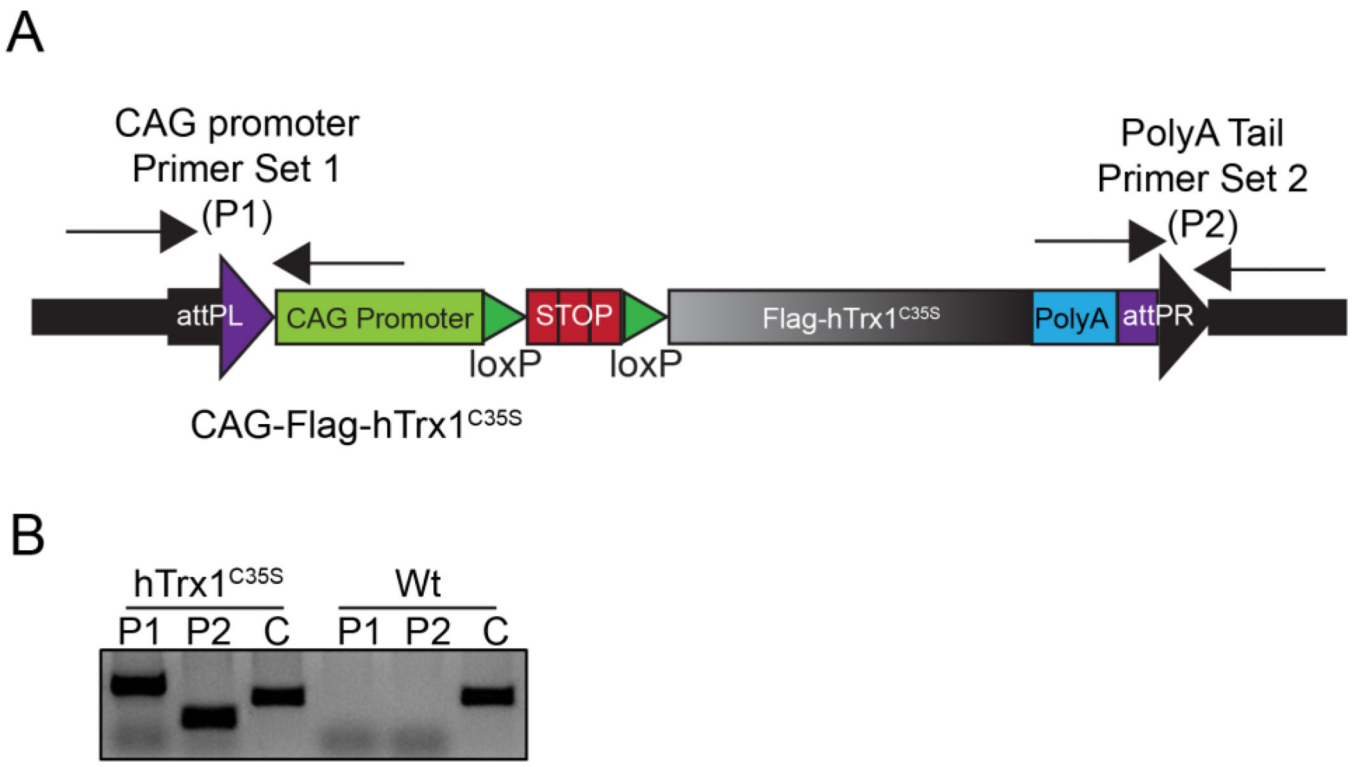

Figure 2.

Schematic of the hTrx1^{C35S} substrate trap mouse gene. (A) Flag-hTrx1^{C35S} was inserted into the Rosa26-3aatP gene in an FVB founder line. (B) Genotyping of the CAG promoter (Lane 1) and the Poly A tail (Lane 2) was successful in the hTrx1^{C35S} transgenic mouse and was not detected in a wild-type mouse. Interleukin-8 served as an internal control (Lane C).

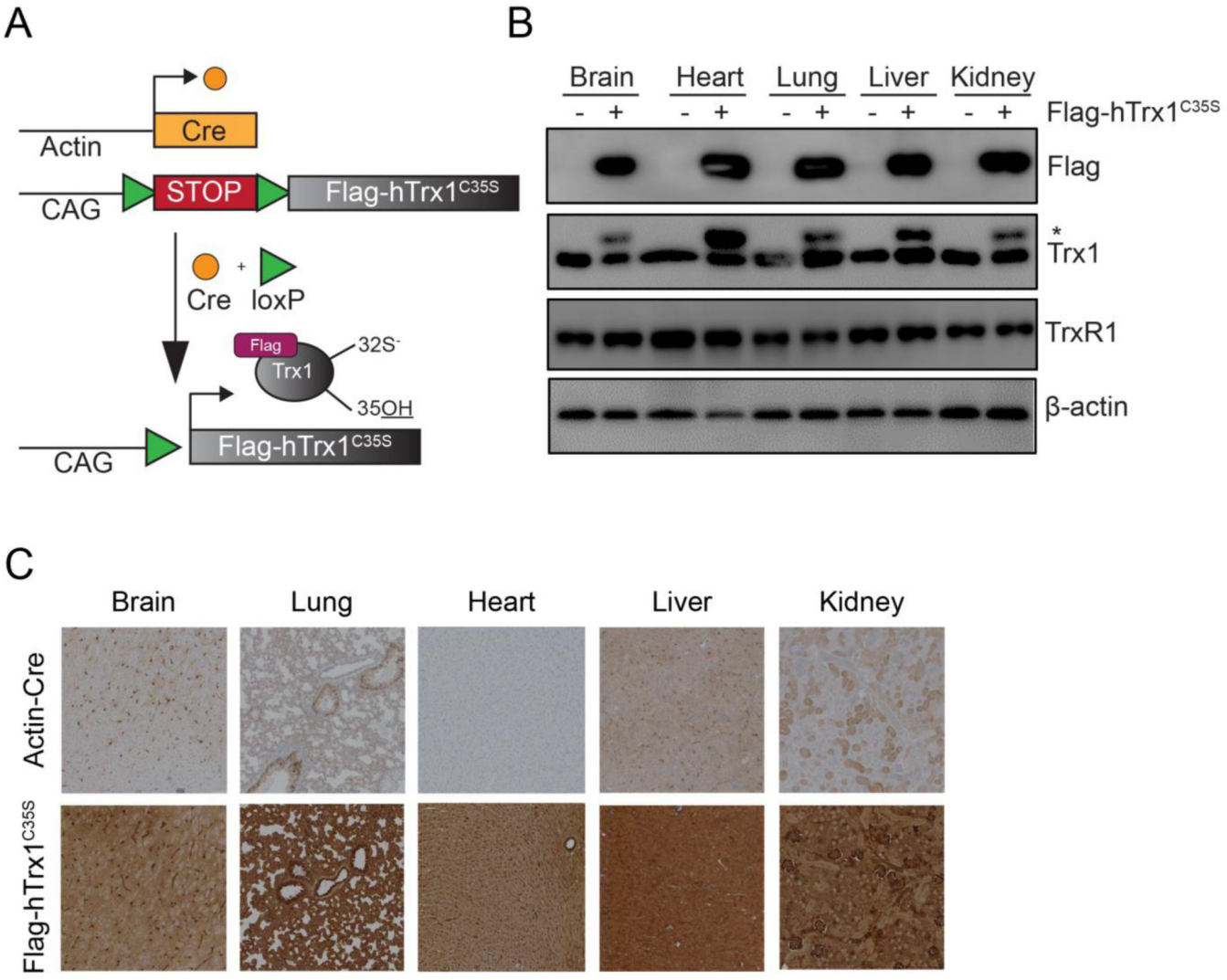

Figure 3.

In vivo expression of the Trx1 substrate trap. (A) Inducible expression of flag-hTrx1^{C35S} in actin-cre;flag-hTrx1^{C35S} mice. Upon cre recombination, the stop sequence is excised and flag-hTrx1^{C35S} protein is expressed. (B) Representative SDS-PAGE/immunoblots of PND5–7 mouse tissues probed for flag, Trx1, and TrxR1 with β-actin as a loading control. hTrx1^{C35S} mice were crossed with mice with cre driven by the actin promoter (actin-cre mice served as controls). The asterisk indicates reduced mobility of the flag-hTrx1^{C35S} protein in comparison to endogenous mouse Trx1. (C) Tissue immunohistochemistry for Trx1 from PND5–7 actin-cre and actin-cre;flag-hTrx1^{C35S} mice.

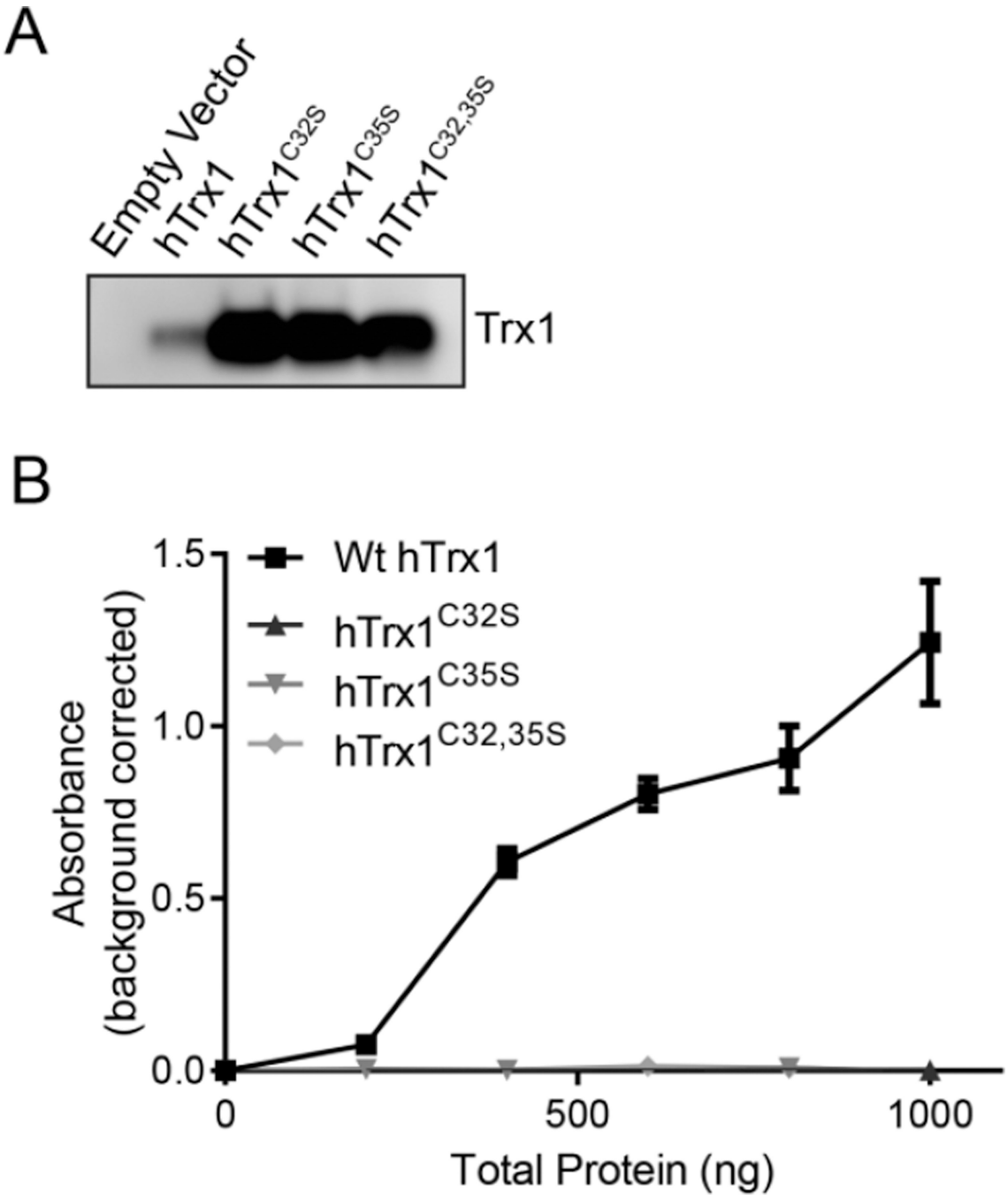

Figure 4.

The Trx1^{C35S} mutation does not exhibit redox activity. Recombinant hTrx1 with specific mutations to cysteines in the catalytic site were expressed in BL21(DE3)pLysS E. coli. (A) Representative SDS-PAGE/immunoblots of recombinant proteins probed with an anti-Trx1 antibody. (B) Thioredoxin activity assay of wild type and mutant recombinant hTrx1.

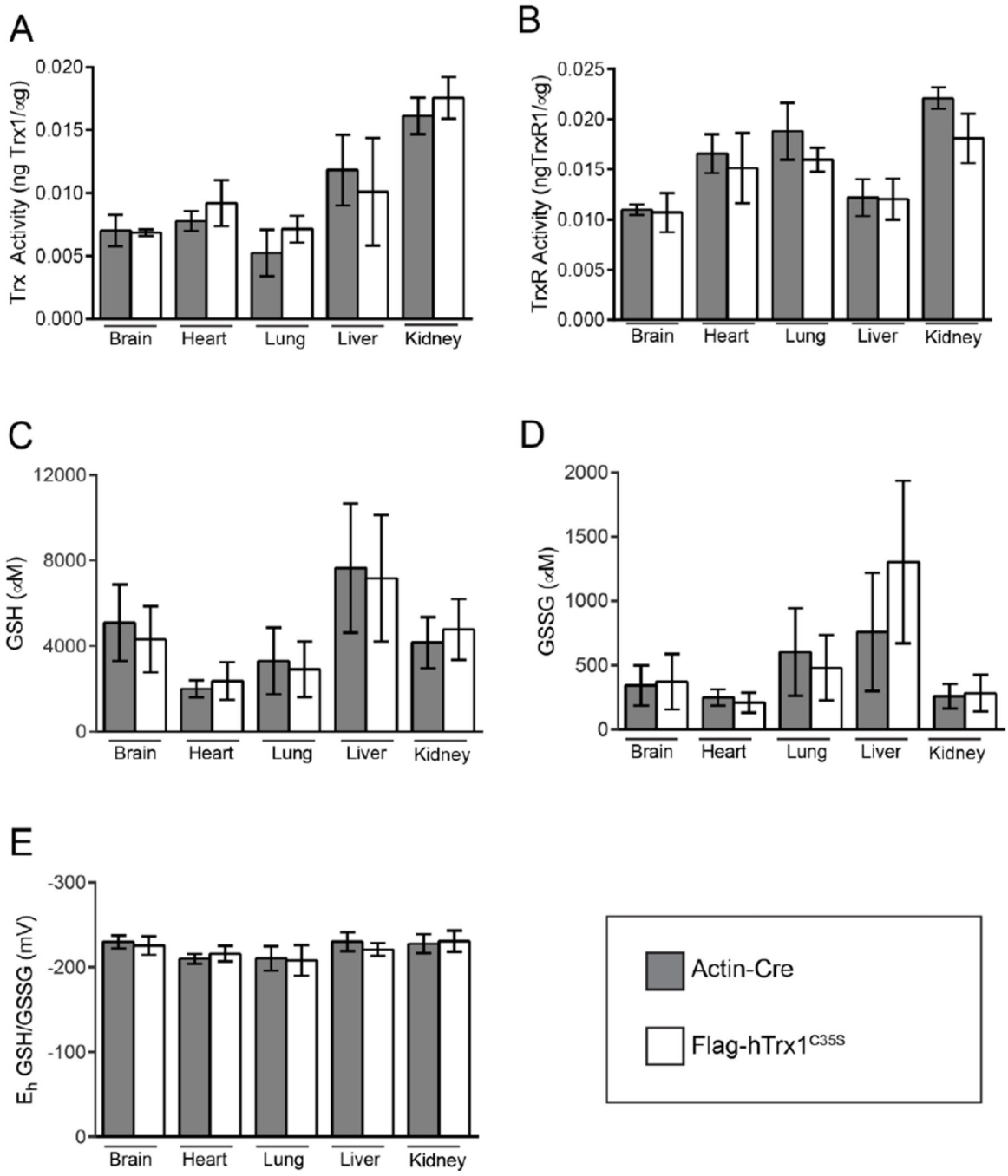

Figure 5.

hTrx1^{C35S} expression does not impair endogenous thioredoxin and glutathione systems. Using a standard insulin reduction assay, endogenous (A) Trx and (B) TrxR activities were measured across tissues from PND5–7 actin-cre control and actin-cre; hTrx1^{C35S} (n=3). (C) Reduced and (D) oxidized glutathione levels and (E) glutathione redox potential in tissues from PND5–7 actin-cre and actin-cre:flag-hTrx1^{C35S} mice. (n=9–10).

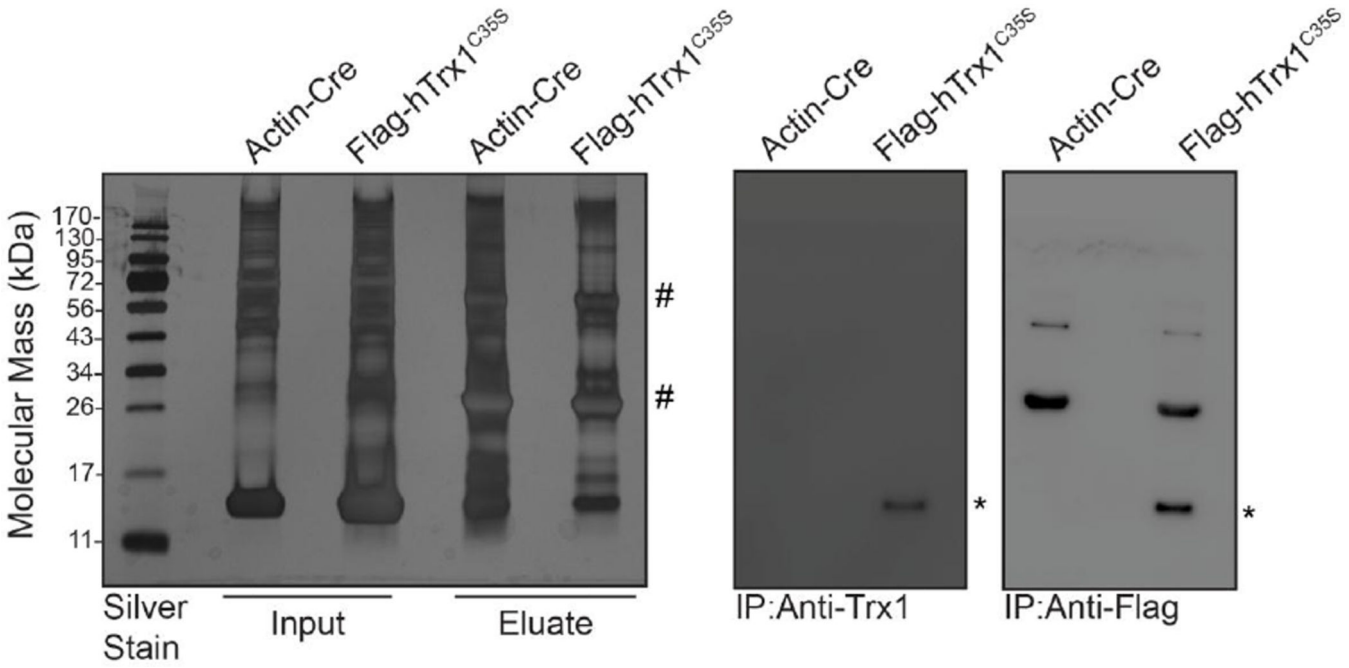

Figure 6.

Immunoprecipitation of hTrx1^{C35S} from lung lysates. Representative silver stain of input and eluate from actin-cre controls and actin-cre;flag-hTrx1^{C35S} mice in room air conditions (n=4). Representative SDS-PAGE/immunoblots of Trx1 and flag in immunopurified eluate. The asterisk indicates detection of the flag-hTrx1^{C35S} transgene. The hash tags indicate the immunoglobulin bands which were removed before mass spectrometry analysis.

Table 1

Homeostatic Trx1 interactions

Name	Abbr.	UniProt	Unique Peptides
14-3-3 protein theta (fragment)	Ywhaz	P6VW30	4
40S ribosomal protein S11	Rps11	P62281	8
40S ribosomal protein S14	Rps14	P62264	5
40S ribosomal protein S15a	Rps15A	P62245	5
40S ribosomal protein S17	Rps17	P63276	5
40S ribosomal protein S19	Rps19	Q9CZX8	10
40S ribosomal protein S4, X	Rps4X	P62702	3
40S ribosomal protein S7	Rps7	P62082	8
60S ribosomal protein L23	Rpl23	P62830	6
78 kDa glucose-related protein	Hspa5	P20029	7
ADP-ribosylation factor 5	Arf5	P84084	3
Cell cycle and apoptosis regulator protein 2	C3	P01027	7
Cysteine and glycine rich protein 1	Csrp1	P97315	10
Collapsin Response Mediator Protein 2	Crmp2	O08553	24
Collapsin Response Mediator Protein 4	Crmp4	E9PWE8	16
EH domain-containing protein 4	Ehd4	Q9EQP2	10
Eukaryotic translation initiation factor 3 subunit M	Eif3m	Q99JX4	5
GTP-binding protein SAR 1a	Sar1a	Q99JZ4	5
Heterogeneous nuclear ribonucleoprotein A3	Hnrnpa3	Q8BG05	6
Heterogeneous nuclear ribonucleoproteins C1/C2	Hnrnpc	Q9Z204	5
Histone H1.2	Hist1h1c	P15864	5
Ig gamma-1 chain C region – secreted	Ighg1	P01869	3
Kinesin-1 heavy chain	Kif5b	Q61768	6
LanC-like protein 2 (fragment)	Lancl2	Q9JJK2	5
Leukocyte elastase inhibitor A	Serpinb1a	Q9D154	7
Myosin light polypeptide 6	Myl6	Q60605	5
Nucleolin	Ncl	P09405	5
Peroxiredoxin 1	Prxn1	P35700	8
Peroxiredoxin 2	Prxn2	Q61171	7
Peroxiredoxin 5	Prxn5	H3BJQ7	5
Plasminogen activator inhibitor 1 RNA-binding protein	Serbp1	Q9CY58	5
Probable ATP-dependent RNA helicase DDX5	Ddx5	Q61656	5
Protein Tns1	Tns1	A0A087WQS0	9
Pulmonary surfactant-associated protein B	Sftpb	P50405	6
Rabankyrin-5	Ankfy1	Q810B6	5
Regulator of nonsense transcripts 1	Upf1	Q9EPU0	5
RNA-binding protein EWS	Ewsr1	Q5SUS9	8
RNA-binding protein Raly	Raly	Q64012	5
Transgelin-2	Tagln2	Q9WVA4	4

Table 2

Hyperoxia-induced Trx1 interactions

Name	Abbr.	UniProt	Unique Peptides
40S ribosomal protein S3a	Rps3a	P97351	7
5-oxoprolinase	Oplah	Q8K010	6
60S ribosomal protein L23	Rpl23	P62830	5
Alpha-2-macroglobulin	Pzp	Q61838	6
Alpha-centractin	Actr1a	P61164	3
ATP-dependent RNA helicase DDX3X	Ddx3x	Q62167	7
Band 3 anion transport protein	Slc4a1	P04919	8
Calumenin	Calu	O35887	6
Capping protein (Actin filament) muscle Z-line, beta, isoform CRA	Capzb	A2AMW0	5
Carbonic anhydrase 2	Ca2	P00920	6
Eukaryotic translation initiation factor 3, subunit E	Eif3e	P60229	9
Eukaryotic translation initiation factor 3, subunit F	Eif3f	Q9DCH4	5
Eukaryotic translation initiation factor 3, subunit L	Eif3l	Q8QZY1	6
Guanine nucleotide-binding protein subunit beta-2-like-1	Gnb2l1	P68040	6
Heterogeneous nuclear ribonucleoprotein A3	Hnrnpa3	A2AL12	4
Kininogen-1	Kng1	D3YTY9	5
Tubulin beta-4B chain	Tubb4b	P68372	3